Proceedings of the ICSC-F'96 Jaszowiec '96

GROWTH OF LASER ABLATED $YBa_2Cu_3O_7$ THIN FILMS EPITAXIED ON (100)MgO: INFLUENCE OF IN-PLANE MISORIENTATIONS ON LOW AND HIGH FREQUENCY PROPERTIES

A. PERRIN, M. GUILLOUX-VIRY AND X. CASTEL
Laboratoire de Chimie du Solide et Inorganique Moléculaire, URA CNRS 1495
Université de Rennes I
Avenue du Général Leclerc, 35042 Rennes-Cedex, France

The graphoepitaxial growth of c-axis $YBa_2Cu_3O_7$ laser ablated thin films on (100)MgO induces a competition between two main in-plane orientations due to the large lattice mismatch: $\langle 100\rangle$ $YBa_2Cu_3O_7$ $\|$ $\langle 100\rangle$ MgO, $c_{\perp 0}$ notation or $\langle 110\rangle$ $YBa_2Cu_3O_7$ $\|$ $\langle 100\rangle$ MgO, $c_{\perp 45}$ notation. The ratio of $c_{\perp 45}/c_{\perp 0}$ in-plane orientations (η), measured by X-ray diffraction φ scans, is ranging from 0.2% to 49.7% for the films reported here. Their crystalline qualities were compared on the basis of rocking curves ($\Delta\theta$), electron channeling patterns and reflection high energy electron diffraction diagrams. The coexistence of $c_{\perp 0}$ and $c_{\perp 45}$ domains creates high angle grain boundaries. No degradation of T_c, residual resistance ratio (RRR) or ΔT_c is observed when η increases. In contrast, a strong correlation between microwave losses characterized by surface resistance (R_S at 10 GHz and 77 K), inductive losses $S(\chi'')$ (surface of the χ'' peak obtained in a.c. susceptibility at 119 Hz) and η was clearly evidenced. A minimum of losses was found for η between 3 and 6% suggesting the necessity of a low quantity of high angle grain boundaries for films optimization. Finally, some specific processes carried out recently in order to try to efficiently control η, then R_S are discussed.

PACS numbers: 68.55.Jk, 81.15.-z, 73.25.+i

1. Introduction

The control of the growth of high quality epitaxial thin films of HTSC materials opens the way to a number of applications, specially in the field of microwave devices. However, working at high frequencies implies additional requirements on the dielectric properties of the substrates and, in this aspect, (100)MgO single crystal is one of the most popular. Unfortunately, this material presents an important misfit with HTSC, meaning severe limitations in the mechanism of heteroepitaxial growth. In this paper, we will focus on the growth of $YBa_2Cu_3O_7$ (YBCO) on (100)MgO using pulsed laser deposition, the specific defects of such films and their implication on the surface resistance R_S which is the pertinent parameter for any microwave applications.

2. Substrates selection

As it will be shown in a later section, microstructural defects have a strong detrimental effect on the surface resistance. Therefore, single-crystal like films are to be used, meaning an epitaxial growth, i.e. specific substrates.

They are a number of structural and chemical strong constraints in selecting these substrates:

— single-crystal materials,

— good unit-cell fit, and in addition atomic positions well fitted in the surface plane,

— stable at high temperature in the presence of oxygen,

— low reactivity with the film material,

— lack of phase transition at or below the processing temperature,

— atomically smooth growth surface.

In addition, several physical properties have to be taken into account, for instance:

TABLE

Summary of structural and physical properties of the most popular substrates for YBaCuO growth.

	MgO (100)	$SrTiO_3$ (100)	$LaAlO_3$ (100)	$NdGaO_3$ (110)	Al_2O_3	$SrLaAlO_4$ (001)	Si (100)
Structure	cubic	cubic	rhombo-hedral	ortho-rombic	hexa-gonal	tetra-gonal	orto-rhombic
Lattice constants [Å]	4.21	3.905	3.79	3.86	4.76	3.77	5.43 (3.84 $\times\sqrt{2}$)
a					12.99	12.63	
b							
c			$\alpha =$ 90°4′		($\alpha_R =$ 86°)		
Misfit YBaCuO [%]	9	1–2	2	0.27	23 10 (R--plane)	2.5	40 0.7
Dielectric constants ε'					9.4 $\perp c$		
(300 K)	9.9	310	20.5–27	23	11.5 $\parallel c$	17	11.6
(100 K)	9.7	2200				16.7	11.4
$\tan\delta$					$8.6 \cdot 10^{-5}$ $\perp c$		
(300 K)	$6.2 \cdot 10^{-6}$	$3 \cdot 10^{-2}$	$3.1 \cdot 10^{-5}$	$7 \cdot 10^{-4}$	$3 \cdot 10^{-5}$ $\parallel c$	$8 \cdot 10^{-4}$	$1 \cdot 10^{-3}$
(100 K)		$6 \cdot 10^{-2}$	$7.6 \cdot 10^{-6}$	$3 \cdot 10^{-4}$	(77 K, 10 GHz)	$2 \cdot 10^{-4}$	$1 \cdot 10^{-4}$
Thermal expansion α (20°C–900°C) (10^{-6}/°C)	8–12	9–11.1	11–12	10	5–7.5	7.5–8.9	4.4

— thermal conductivity and thermal expansion factors, — dielectric properties: for microwave applications ε' must not be too high, in particular for modelling and miniaturization problems, and ε'' (losses) has to be as low as possible.

Finally, availability and price are also of importance for the future.

Table summarizes the properties of a number of substrate materials. Si and Al_2O_3 are chemically reactive and generally need buffer layers. The perovskite $SrTiO_3$ is an excellent compromise for low frequency applications, but presents unacceptable losses in microwave field. For the latter applications, $LaAlO_3$ is a good candidate with a small lattice mismatch. However, for frequencies larger than 20 GHz, its dielectric constant becomes too high. Moreover, $LaAlO_3$ is quite expensive and twinned. Finally, MgO is still the most popular substrate in spite of the large misfit (8%) with *c*-axis oriented YBaCuO.

3. Growth of YBCO on (100)MgO

The unit-cell mismatch between MgO and YBCO is not compatible with a true heteroepitaxial growth, leading to specific defects and growth mechanisms.

3.1. Growth mode

The first stage of nucleation and growth of YBCO on (100)MgO is a 3D island mechanism, as clearly shown recently by Lesueur et al. [1] and Hüttner et al. [2]. Rutherford backscattering analyses of ultrathin films give an apparent thickness largely higher than the average value calculated from the deposition rate, meaning the formation of island instead of an even coverage. This result strongly contrasts with the data obtained on similar films grown on $SrTiO_3$ substrates, for which the expected and effective thicknesses agree closely. These conclusions have also been confirmed by the analysis of X-ray diffraction (XRD) peaks broadening in the frame of the Scherrer model [3]. In a further stage, growth proceeds from steps and dislocations, giving the classical spirals well illustrated by atomic force microscopy (AFM) and scanning tunneling microscopy (STM) [4]. As shown by stress measurements, the films grown on $SrTiO_3$ are under compression in the (*a*, *b*) plane whereas the ones grown on MgO are on extension [5]. This behavior accords with the mismatch values for these two different substrates.

3.2. Graphoepitaxy

This 3D Volmer–Weber model initial growth is of course related to the unit-cell mismatch, as the substrate network cannot run continuously into the film [6]. However, at the interface, the Coulombic periodic potential of both the film and the substrate tends to be accorded, as far as possible. As the two networks are noncommensurate, coincidence of a given site occurs only after a certain number of unit-cell translations, defining a surface Σ (the inverse of which is defined as the density of near site lattice coincidences) and the efficiency of matching of the two networks as [7]

$$f = \frac{2|\Sigma_S^{1/2} a_S - \Sigma_F^{1/2} a_F|}{\Sigma_S^{1/2} a_S + \Sigma_F^{1/2} a_F}.$$

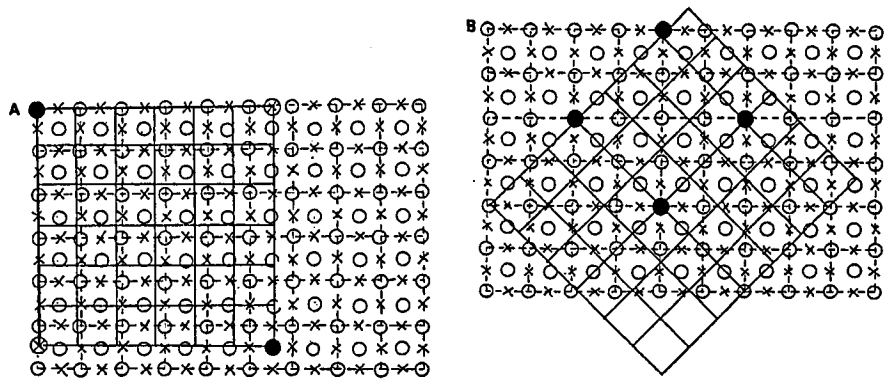

Fig. 1. In-plane schematic representation from MgO cubic lattice (dashed line) and YBaCuO lattice (full line), giving evidence of the near coincidence sites lattice (black circles) in the particular cases of the $c_{\perp 0}$ (A) and of the $c_{\perp 45}$ (B) orientations [19].

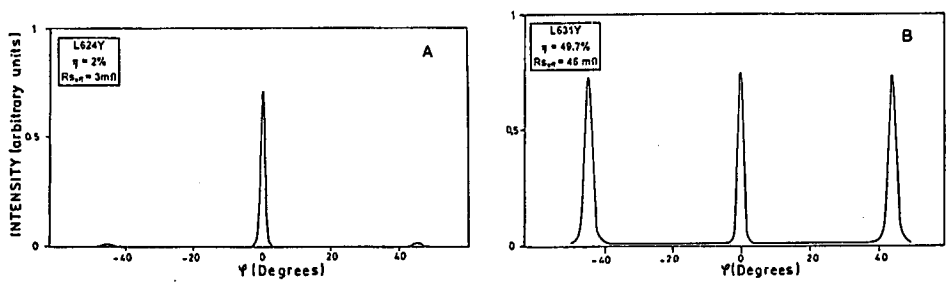

Fig. 2. X-rays φ scans of the (103)YBaCuO peak for two films deposited by laser ablation on (100)MgO presenting a mixed orientation $c_{\perp 0}$ and $c_{\perp 45}$ of 2% (A) and 49.7% (B).

Figures 1A and 1B schematize some possible coincidences of the networks of c-oriented YBCO and (100)MgO. In fact, a given situation is stable if Σ is not too large and if (the misfit of the "superlattices" at the interface) is very small. This is reasonably the case for the represented situations and, in fact, the so-called $c_{\perp 0}$ and $c_{\perp 45}$ are currently encountered in the case of c-axis YBCO grown on (100)MgO. The two orientations often coexist, as early shown by Weissenberg photographs [8] and AFM/STM microscopies [4].

In a mixed film, the occurrence of the two orientations can be quantitatively measured by the use of a four circle X-ray texture diffractometer. As an example, Fig. 2 reproduces the φ scans around the (103)/(013) planes, which are tilted by about 45° with respect to the substrate surface for typical samples [9]. Peaks at 0°, 90° and 270° arise from domains where the unit-cell vectors of the film and the substrate are aligned, peaks at 45°, 135° and 225° are related to 45° rotated domains. The ratio η of the two families is deduced from the relative intensities by

$$\eta = \frac{I_{103}(\varphi_{45})}{I_{103}(\varphi_0) + I_{103}(\varphi_{45})} \times 100.$$

3.3. Induced specific defects

At the vertical interface between two differently oriented domains is a discontinuity in the atomic periodicity of the network, called a high angle grain boundary (HAGB) by contrast with low angle grain boundaries where two successive grains have their networks aligned. In pulsed laser deposition grown films, the lateral dimension of individual grains (visualized by the spiral features) is typically 1000–2000 Å, so the *density* of HAGB will be proportional to the relative occurrence of one orientation versus the other one.

3.4. Effect of deposition parameters on film orientation

It is well admitted that the deposition temperature has a strong effect on the out-of-plane growth: lowering the substrate temperature favors *a*-axis orientation, whereas higher temperatures allow the growth of purely *c*-axis oriented films.

The effect of deposition parameters on in-plane orientation is not so evident. For instance, Fig. 3a reproduces the results of Keller et al. [10], showing a temperature window about 40°C wide giving almost pure $c_{\perp 0}$ orientation. At higher temperature $c_{\perp 45}$ orientation starts to appear. However, Fig. 3b reports a number

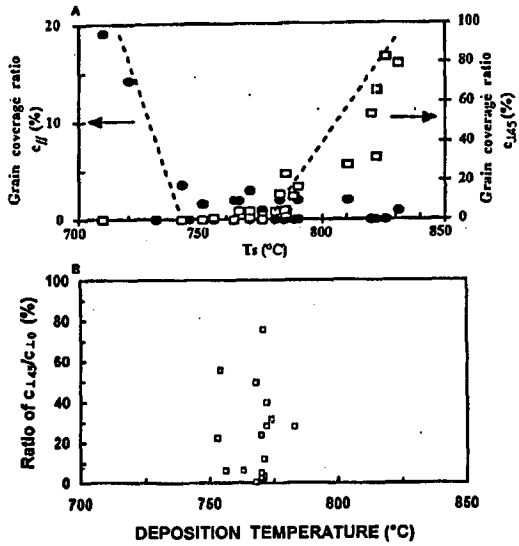

Fig. 3. Ratio of the mixed orientation $c_{\perp 0}$ and $c_{\perp 45}$ versus the deposition temperature: results reported by two different groups in (A) [10] and (B) [this work] showing that a correlation between the deposition parameters and the in-plane ordering on MgO is not self-evident.

of data obtained in a similar deposition temperature range. One can notice a large spread of $c_{\perp 45}/c_{\perp 0}$ ratio. Moreover, a set of 13 films, deposited exactly in the same conditions (temperature, pressure, distance and fluence) shows also an important spread of in-plane orientation. This result suggests a strong influence of additional parameter, like some difference in substrate surface. As all the substrates used in this series were coming from the same batch, it is thought that the differences would be very subtle.

Indeed, Moeckly et al. [11] have previously reported the influence on in-plane orientation of various substrate's surface treatment (chemical or mechanical polishing, high temperature annealing) but we could not reproduce their results. Specific treatments of substrates have been reported and will be discussed in a following section.

4. Surface resistance R_S of YBCO/MgO films

As stated above, the pertinent parameter for any application of thin films in the field of microwaves is the surface resistance R_S, because zero resistance in superconductors is reached only at zero or very low frequency.

4.1. R_S measurements

Surface resistance measurements request very specific devices with often strong geometrical constraints which are even more complicated by the cryogenic environment.

A complete general survey of various techniques has been recently reported by Zhen [12]. Shortly, they include:

— the patterned transmission line method,
— the cylindrical or conical resonant cavities,
— the parallel plates method,
— the confocal reflectometer method,
— the transmitted power measurements in waveguides [13],
— the dielectric resonator.

However, the first method is destructive, the second needs large films, the third requests two films, the fourth is specially adapted to mapping R_S in the case of large sized films and the fifth is restricted to very thin films grown on substrates well sized with respect to the guide dimensions. The dielectric resonator method [14] has the advantages to be non-destructive and to have no strong geometrical constraints.

4.2. Correlations between R_S and other properties

Because of the difficulty to measure routinely R_S, it is of interest to try to correlate the surface resistance with other structural and/or physical properties more systematically accessible.

4.2.1. R_S and microstructure: HAGB density

According to theoretical models, R_S would be sensitive to any local depression of the order parameter, induced for instance by structural defects.

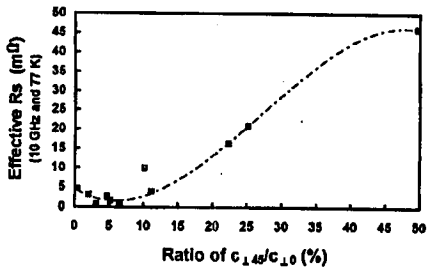

Fig. 4. Effective surface resistance R_S measured at 10 GHz and 77 K versus the ratio of the two in-plane orientations.

Therefore one can expect a strong correlation between R_S and the HAGB density as stated previously, the latter being directly related to the $\eta = c_{\perp 45}/c_{\perp 0}$ surfaces ratio [15] which in turn is quantitatively measured by XRD diffraction in off-angle φ scan mode.

Figure 4 reports R_S as a function of η for a number of YBCO films c-axis grown on (100)MgO substrates. The value of η is limited to 50% for symmetrization (and indeed 100% pure $c_{\perp 0}$ and $c_{\perp 45}$ films exhibit similar R_S values [16]).

As expected, a very strong correlation is evidenced. However, an unreported feature (although discernible in data reported in [17]) is the R_S minimum occurring near $\eta = 3\%$. Obviously, the large increase in R_S for larger values of η is directly related to an increase in HAGB density and can be interpreted by adding an additional term in the Hylton model [18] in order to account for this specific type of defects [9]. The decrease in R_S for η up to 3% can be understood in the frame of the two fluid model as the effect of the decrease in the relaxation time τ (reduced by the presence of a low density of defects) which in turn decreases σ_1, the real part of the complex conductivity.

No correlation has been observed between R_S and the FWHM of $\Delta\theta$, the broadening of XRD rocking curves around 001 diffractions, although the latter contains a term related to the crystalline coherence in the film plane.

4.2.2. R_S and physical properties

The surface resistance R_S has been studied as a function of T_c for a number of films, some of them having been grown in non-optimized conditions. There is no noticeable correlation excepted the appearance of a threshold value, and indeed, the films having very low T_c exhibit high R_S [16, 19]. However, the same plot for optimized samples exhibits only a randomly spread cloud of points. Therefore, there is not any correlation between T_c and R_S, at least for optimized films.

Similarly, the measurements of standard data such as the RRR, ΔT_c, $\Delta\chi'' \ldots$, are not able to give any prediction about the expectable R_S values.

It is established [20] that R_S correlates to J_c, the critical current density, because structural defects are deleterious in a similar way for these two data. Also, the absolute value of the normal state resistivity would be a good indication of the film quality. However, for high precision, these measurements need the patterning of the film and are destructive: so they have not been selected in the search of correlations.

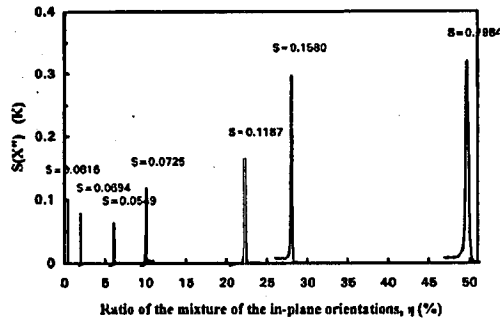

Fig. 5. Evolution of the χ'' peak with in-plane orientation in YBaCuO thin films grown on (100)MgO. The numerical values correspond to the effective area under the curve of the dissipative contribution χ'', normalized to the χ' amplitude.

In contrast, a.c. susceptibility measurements are non-destructive and are quite flexible about the size and thickness of the films (at least using a home-made equipment). As displayed in Fig. 5, the losses, represented by the χ'' peak, clearly increase when the η parameter increases. More quantitatively, we have also reported in Fig. 3 the numerical values of the area $S(\chi'')$ of the χ'' peak, normalized by the amplitude of the χ' step to take into account geometrical factors, as a function of the η parameter. These data clearly correlate and, in addition, the shape of the curves $R_S = f(\eta)$ and $S(\chi'') = f(\eta)$ behaves very close, leading to a linear relationship between R_S and $S(\chi'')$.

Finally, in order to evaluate the quality of a YBCO/MgO thin film to be used in the microwave field, the above correlations give three independent methods belonging to different fields of materials sciences:

— direct R_S measurement (electronics),
— structural data (crystallography),
— a.c. susceptibility (physics).

5. How to control R_S?

As stated above, the obtention of low R_S values is directly related to the control of low HAGB density. The growth conditions, for instance the substrate temperature, can have some influence, but other parameters, related to substrate surface quality, appear determinant.

Indeed, the experiments of Moeckly et al. [11] have suggested such an effect: from pole figures analyses, they have reported that films grown on chemically polished substrates gave a mixture of several in-plane orientations whereas mechanically polished substrates and, even more clearly, annealed substrates, tend to give unique $c_{\perp 0}$ orientation. This result could be related to the formation, at the substrate surface, of steps favorable to a lateral growth, as shown by a very recent AFM comparative study of YBCO films grown on either untreated or 1200°C annealed (100)MgO substrates [21]. In addition, the promoted quick lateral growth induces a quick coalescence, leading to substantially smoother YBCO film surface.

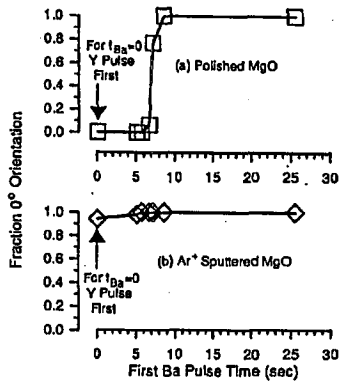

Fig. 6. (a) YBaCuO in-plane orientation on epitaxially polished MgO as a function of first Ba pulse time and (b) YBaCuO in-plane orientation on Ar^+ sputtered MgO as a function of first Ba pulse time. (Reprinted with permission from [22]. Copyright 1996 American Institute of Physics).

Another way to modify the substrate surface has been recently reported by Buchholz et al. [22]. Prior to deposition of YBCO, a seed layer of BaO was grown *in situ*. For low BaO coverage (typically one or less monolayer) $c_{\perp 45}$ orientation is obtained, whereas at higher BaO coverage pure $c_{\perp 0}$ orientation is observed (Fig. 6a). According to Cotter et al. [23], Ba is substitutionally incorporated into the MgO lattice for coverage less than two monolayers, and, in contrast, forms an epitaxial overlayer when the thickness is three monolayers or more.

In addition, a slight etching of MgO surface using Ar^+ ions promoted the $c_{\perp 0}$ orientation whatever the thickness of the BaO seed-layer (Fig. 6b). Interestingly, this behavior can be compared to the results we have previously obtained when growing YBCO on bare sapphire substrates, i.e. without any buffer layers: untreated substrates lead to textured YBCO films, whereas ion milled ones gave epitaxially grown films with T_c as high as 88 K [24].

The ion bombardment is expected to provoke vacancies, ledges and kink sites on the substrate surface [25]. However, in both the processes reported above, the ion milling was carried out *ex situ* several hours or even several days [26] before the film growth and the substrates were exposed to atmosphere. Therefore, the active site would have been destroyed and the actual effect of the treatment is, in our opinion, still to be explained.

6. Concluding remarks

In summary, the detrimental effect on surface resistance of high angle grain boundaries in YBCO films grown on (100)MgO was illustrated. These HAGB are related to the large mismatch between the film and the substrate and can be explained in the frame of the near site coincidence lattice model. As they act as weak links, they tend to quickly increase the surface resistance of films, at least when their density becomes important. This density is difficult to control, although some specific treatments of substrate surface appear promising.

Of course, an alternative way to rule out the HAGB is the use of well matched substrates meanwhile some other disadvantages. The use of CeO_2 buffered R-plane sapphire [27, 28] for instance, could be developed: the attainable quality of very thin (less than 100 Å) buffer layers is excellent as attested by the observation of Laue oscillations and remarkably small mosaic effects.

References

[1] J. Lesueur, M. Aprili, T.J. Horton, F. Lalu, M. Guilloux-Viry, A. Perrin, L. Dumoulin, *E-MRS 96 Symposium F*, to appear in *J. Alloys Comp.*

[2] D. Hüttner, U. Günther, O. Meyer, J. Reiner, G. Linker, *Appl. Phys. Lett.* **65**, 2863 (1994).

[3] G. Linker, D. Hüttner, O. Meyer, M. Ohkubo, G. Reiner, *E-MRS 96 Symposium F*, to appear in *J. Alloys Comp.*

[4] I.D. Raistrick, M. Hawley, *Physica D* **66**, 172 (1993).

[5] S. Auzary, F. Badawi, L. Bimbault, J. Rabier, R.J. Gaboriaud, *E-MRS 96 Symposium F*, to appear in *J. Alloys Comp.*

[6] N. Savvides, A. Katsaros, *Physica C* **226**, 23 (1994).

[7] D.M. Hwang, T.S. Ravi, R. Ramesh, Siu-Wai Chan, C.Y. Chen, L. Nazar, X.D. Wu, A. Inam, T. Venkatesan, *Appl. Phys. Lett.* **57**, 1690 (1990).

[8] A. Perrin, M.G. Karkut, M. Guilloux-Viry, M. Sergent, *Appl. Phys. Lett.* **58**, 412 (1991).

[9] X. Castel, M. Guilloux-Viry, A. Perrin, C. Le Paven-Thivet, J. Debuigne, *Physica C* **255**, 281 (1995).

[10] D. Keller, A. Gervais, D. Chambonnet, C. Belouet, C. Audry, *J. Phys. III (France)* **5**, 135 (1995).

[11] B.H. Moeckly, S.E. Russek, D.K. Lathrop, R.A. Buhrman, Jian Li, J.W. Mayer, *Appl. Phys. Lett.* **57**, 1687 (1990).

[12] Z.Y. Zhen, *High Temperature Superconducting Microwave Circuits*, Artech House, Norwood (MA) 1994.

[13] F. Mehri, P. Leperc, J.C. Corru, E. Playez, C. Thivet, A. Perrin, D. Chambonnet, *J. Phys. III (France)* **4**, 2259 (1994).

[14] J.C. Mage, B. Marcilhac, M. Mercandalli, Y. Lemaître, S. Barrau, D. Dessertennes, D. Mansart, J.P. Castera, P. Hartemann, *J. Phys. III (France)* **4**, 1285 (1994).

[15] S.S. Laderman, R.C. Taber, R.D. Jacowitz, J.L. Moll, C.B. Eom, T.L. Hylton, A.F. Marshall, T.H. Geballe, M.R. Beasley, *Phys. Rev. B* **43**, 2922 (1991).

[16] C. Le Paven-Thivet, M. Guilloux-Viry, J. Padiou, A. Perrin, M. Sergent, L.A. de Vaulchier, N. Bontemps, *Physica C* **244**, 231 (1995).

[17] M. Schieber, Y. Ariel, A. Raizman, S. Rotter, *Appl. Superconductivity* **1**, 827 (1993).

[18] T.L. Hylton, A. Kapitulnik, M.R. Beasley, J.P. Carini, L. Drabek, G. Grüner, *Appl. Phys. Lett.* **53**, 1343 (1988).

[19] C. Le Paven-Thivet, Ph.D. Thesis, University of Rennes I, France 1994.

[20] W. Rauch, E. Gornik, G. Söltner, A.A. Valenzuala, F. Fox, H. Behner, *J. Appl. Phys.* **73**, 1866 (1993).

[21] M. Ye, M.P. Delplanck, R. Deltour, R. Winand, *Mater. Sci. Eng. B*, 1997, in press.

[22] D.B. Buchholz, J.S. Lei, S. Mahajan, P.R. Markworth, R.P.H. Chang, B. Hinds, T.J. Marks, J.L. Schindler, C.R. Kannewurf, Y. Huang, K.L. Merkle, *Appl. Phys. Lett.* **68**, 3037 (1996).

[23] M. Cotter, S. Campbell, R.G. Egdell, W.C. Mackrodt, *Surf. Sci.* **197**, 208 (1988).

[24] C. Thivet, M. Guilloux-Viry, J. Padiou, A. Perrin, G. Dousselin, Y. Pellan, M. Sergent, *Physica C* **235-240**, 665 (1994).

[25] M.B. Gusera, V.V. Khovostov, B.M. Kosishko, S.Ju. Kovalenko, *Surf. Sci. Lett.* **276**, L24 (1992).

[26] R.P.H. Chang, private communication.

[27] M. Maul, B. Schulte, P. Häussler, G. Frank, T. Steinborg, H. Fuess, H. Adrian, *Appl. Phys. Lett.* **74**, 2942 (1993).

[28] M.W. Denhoff, J.P. McCaffrey, *Appl. Phys. Lett.* **70**, 3986 (1991).